11-10-2006

Histone acetylation and expression of SMN, the spinal muscular atrophy gene

Lauren Kernochan

Histone acetylation and expression of *SMN*, the spinal muscular atrophy gene

A Thesis Submitted to the
Yale University School of Medicine
in Partial Fulfillment of the Requirements for the
Degree of Doctor of Medicine

by
Lauren E. Kernochan
2006

HISTONE ACETYLATION AND EXPRESSION OF *SURVIVAL OF MOTOR NEURON* (*SMN*), THE SPINAL MUSCULAR ATROPHY GENE.

Lauren E. Kernochan, Nathan S. Woodling, Thanh N. Huynh, Amy M. Avila, Kenneth H. Fischbeck, Charlotte J. Sumner. Neurogenetics Branch, National Institute of Neurologic Disorders and Stroke, National Institutes of Health, Bethesda, MD. (Sponsored by Stephen M. Strittmatter, Department of Neurology, Yale University School of Medicine, New Haven, CT)

Abstract

Spinal Muscular Atrophy (SMA) is an inherited neuromuscular disorder caused by mutation of the *Survival Motor Neuron* (*SMN1*) gene. Embryonic lethality is rescued by a nearly identical copy of the gene, *SMN2*, which exists in variable copy number and produces a small quantity of functional SMN protein. Because disease severity inversely correlates with *SMN2* gene copy number and with SMN protein level, one therapeutic strategy has been to increase *SMN2* expression. Previous investigators have demonstrated that *SMN* promoter activity, transcript, and SMN protein are increased in cells treated with histone deacetylase (HDAC) inhibitors, suggesting a role for histone acetylation in the regulation of *SMN* expression.

To further investigate epigenetic regulation of *SMN*, we used chromatin immunoprecipitation to characterize the acetylation state of histones associated with the *SMN* promoter locus. We show that the *SMN* promoter has a reproducible pattern of histone acetylation conserved across species and tissues.

Following treatment with HDAC inhibitors, we correlated a 2-fold increase in *SMN* promoter activity, with an increase in H3 and H4 histone acetylation, particularly in upstream regions 2-3 kb from the translational initiation site. During development in mouse tissues, SMN transcript decreased 40-60%, correlating with a decrease in histone acetylation levels within the region closest to the transcriptional start site. These data indicate that histone acetylation is a biologically relevant determinant of *SMN* gene expression, and that this epigenetic variable can be manipulated pharmacologically.

Acknowledgements

I would like to thank Drs. Kenneth Fischbeck and Charlotte Sumner, for their scientific passion, knowledge and diligence, as well as for their unwavering support and encouragement. I thank Dr. Strittmatter for his writing assistance and support. I would like to thank the Howard Hughes Medical Institute, and in particular the staff of the Cloister Scholar Program, for financially supporting me during this work, and for their encouragement of physician scientists. Yale University is acknowledged for their support of science as an important component of medical education. The Cha lab, and Ann Dean are acknowledged for their assistance with chromatin immunoprecipitation methodology and data analysis.

I would particularly like to thank everyone in the Fischbeck lab and Neurogenetics Branch of the NINDS, NIH for their technical support and for their encouragement. Nathan S. Woodling is acknowledged for his experimental expertise, as well as former HHMI scholar Thanh Huynh for her efforts in developing the ChIP protocol.

I would also like to thank my family for their support of whatever the heck it is I do, and in particular my dear godfather Joseph Helms for his honest advice and kind humor. Thank you to Matthew Husa for his faith in me.

Table of Contents

1. Introduction ……... 4

2. Statement of purpose …….. 10

3. Methods……..……..... 12

4. Results……..…. 20

5. Discussion ……..……. 27

6. References …… 35

7. Figures……..….. 40

Introduction

Spinal muscular atrophy (SMA) is an autosomal recessive neuromuscular disease for which there is currently no treatment. It is the leading inherited cause of infant mortality with an incidence of 1 in 6-10,000 live births and a carrier frequency of 1-2% (1-3). Clinically, SMA is characterized by profound muscle weakness in a symmetrical distribution, with proximal muscles more affected than distal, and lower extremities more than upper. In addition to weakness, patients often exhibit hypotonia, hyporeflexia and tongue fasciculations (1). In contrast to patients with other neurodegenerative diseases such as amyotrophic lateral sclerosis (ALS), the disease course is generally not progressive. Patients with SMA show little or no decline in objective muscle strength after an initial phase of decline (1, 4). Pathologic analysis of spinal cord and muscle from human autopsies and mouse models of SMA show a pattern of axonal degeneration with subsequent denervation of muscle fibers, although it is not clear that particular groups of motor neurons are disproportionately affected (5, 6).

SMA is clinically divided into three forms. SMA type I, or Werndig-Hoffman disease, is the most severe form and accounts for over 50% of cases. These patients present within the first six months of life, are never able to sit unaided, and die by the age of 2 years. In the most severe of these cases, mothers will feel a cessation of fetal movement before birth and the infants will die within the first few months of life. Type II patients experience the onset of

symptoms within the first 18 months of life, are able to sit but not stand unaided, and can live into early adulthood. Type III patients present later, can have a normal lifespan, and are able sit and stand unaided at some point in their lives, although they are usually wheelchair bound. Interestingly, patients will usually develop normally at first, then plateau, failing to attain developmental milestones of strength, rather than experiencing a significant loss of strength. The primary source of mortality in all patients is respiratory failure due to weakness of the muscles of inspiration (1, 7).

Spinal muscular atrophy is caused by deletion or mutation of the *Survival Motor Neuron* (*SMN1*) gene, located at 5q13 (8). An inverted near duplicate of the gene, *SMN2*, is present in variable copy number centromeric to *SMN1*. Due to a C to T base change in a splice-enhancing region of *SMN2*, 70-85% of the mRNA produced from *SMN2* is lacking exon 7 (9). The protein produced from the truncated SMN2 mRNA is unstable and thought to be rapidly degraded (10). A small fraction of the mRNA produced from *SMN2* (15-30%) is full length and codes for a fully functional SMN protein, providing enough SMN for cell survival, and to prevent the early embryonic lethality seen in species lacking *SMN2*. Not surprisingly, severity of symptoms in spinal muscular atrophy is inversely correlated with *SMN2* copy number, and with the amount of SMN protein present in the spinal cord (11).

SMN is a ubiquitously expressed protein with a well-established function in splicing (12, 13) and a putative role in mRNA transport (14, 15). SMN is present and necessary for survival in all cells, evoking the question of why motor neurons

are uniquely sensitive to low levels of SMN. The SMN complex, composed of SMN and at least 6 gemin proteins, plays an essential role in assembly of small nuclear ribonucleoproteins (snRNPs). SMN has binding sites for gemin-2 (formerly SMN interacting protein-1 or SIP-1) and for RNA. It is found primarily in the nucleus in discrete “gems”, for gemini of coiled bodies, and is also found at the nucleolar membrane and diffusely within the nucleoplasm and cytoplasm (12). More recently, SMN has been visualized at the leading edge of motor neuron growth cones (16) and has been shown to associate with the mRNA of β-actin, suggesting a role for SMN in the enrichment of particular mRNAs necessary for developing growth cones (14, 15).

When observed under the microscope, affected motoneurons from mouse models of SMA and from human autopsies display the typical “ballooning” phenotype of degenerating neurons (5, 6, 17). Accumulations of neurofilaments have been described, consistent with the hypothesis that cytoskeletal disorganization contributes to the pathogenesis of SMA (6). Reduced synaptophysin staining is also observed in affected motoneurons suggesting a loss of synaptic contact (5). Muscle biopsies in SMA can vary widely depending on disease severity. In adults with type III SMA, fibers show typical neuropathic changes with fibers that are atrophic and band or triangular shaped in cross section, and grouping of type 1 and 2 fibers indicating reinnervation. In a child with type I SMA, fibers are smaller in diameter than normal but remain circular, without the fiber type-grouping pattern seen with reinnervation. These patterns have been correlated electrophysiologically (5, 6).

Because of its early onset and lack of significant progression, SMA has been postulated to be a disease of development. In normal individuals, SMN protein has been shown to be highly expressed during development, with a dramatic decrease in the post-natal period and into adulthood (18). In embryonic chick P19 cells, cellular differentiation to a mature neuronal phenotype is also associated with a decrease in SMN levels (19). Knockdown of SMN mRNA in a zebrafish model was found to impair motor axon outgrowth and pathfinding (20). Taken together, these data suggest that SMN may play a role in neuronal development, and that SMA may in fact be a developmental disorder. It has been postulated that in affected individuals, developmental down-regulation of the gene causes SMN protein levels to fall below some absolute threshold, resulting in lack of viability in developing motor neurons, and the cessation of further development in motor strength.

Since the recognition that SMA is caused by a lack of SMN protein, increasing *SMN2* expression has become one of the most promising strategies for treatment of SMA (21). The finding that histone deacetylase inhibitors can increase *SMN2* expression *in vitro*, suggested that histone acetylation, an important epigenetic determinant of gene expression, might play a role in *SMN2* expression. Histone deacetylases (HDACs), in conjunction with histone acetyltransferases (HATs), control the balance of acetylation of histone H3 and H4 “tails” (22). Increased histone acetylation has been correlated with increased gene expression, and decreased acetylation with decreased gene expression (22, 23). This was thought to be due to repel forces between the acetyl groups

and the negatively charged phosphate backbone of the DNA, creating more space at the site of transcription binding. More recently, a “histone code” has been described in which modifications (acetylation, methylation, phosphorylation, and sumoylation) of particular residues on histone amino terminus tails create a template for transcription factor binding within a gene’s promoter (24). Inhibitors of HDACs have been shown to increase global histone acetylation, and to alter expression in approximately 2% of genes (25). Several groups have shown that compounds which inhibit histone deacetylases can increase *SMN2* expression *in vitro* (26-29) and improve survival *in vivo* (28). Despite their relative nonspecificity, HDAC inhibitors are now being evaluated in limited clinical trials for use in SMA (21).

Currently available HDAC inhibitors are known to act on most of the 10 individual HDACs from classes I and II that have been identified to date. Class I HDACs, including HDACs 1,2,3, and 8, are similar to the yeast RPD3 protein, and localize primarily to the nucleus. Class II HDACs, including HDACs 4,5,6,7,9 and 10, are similar to the yeast HDA1 protein, and localize to both the nucleus and the cytoplasm. Class III HDACs are the most structurally distinct. They are NAD-dependent enzymes similar to the yeast SIR2 proteins, and are not susceptible to inhibition by Trichostatin A, the prototypical HDAC inhibitor (30).

HDACs are thought to increase *SMN* expression by activating the *SMN* promoter. The human *SMN1* and *SMN2* promoters are nearly identical in sequence and activity (9, 19, 31), with a principal transcriptional initiation site located 163 bp upstream of the translational initiation site. Recently, a second

transcriptional initiation site used during fetal development and in undifferentiated P19 cells, has been identified at 242 bp, 79 bp upstream of the primary site (32). The *SMN* promoter was originally thought to encompass a 3.4kb region (19), but recent data suggests that all the elements needed for activation are present within the first 180bp. Sequences with negative regulatory activity have, however, been found as far as 4.6 kb from the translational initiation site (33). Mice have a single *Smn* gene, analogous to our *SMN1*, which shares sequence homology with the human *SMN* promoters (33, 34). Transcription factor analysis shows likely binding sites for a number of factors, including Sp1, CREB and YY1 (31). Recently, Sp and Ets cis-elements, working in combination, have been shown to promote activation in neuronally differentiated P19 cells (32).

Statement of purpose, specific hypothesis, and specific aims of the thesis

The purpose of our study was to investigate the role of histone acetylation in expression of *SMN*. We hypothesized that histone acetylation would have a consistent baseline pattern along the promoter, likely with an increase in acetylation close to the site of transcription initiation, as described at other gene site (35, 36). We also hypothesized that an increase in histone acetylation within the promoter would correlate with an increase in *SMN* promoter activation and gene expression, and that this effect would be both biologically significant and vulnerable to pharmacologic manipulation.

Specifically, our first aim was to characterize the baseline histone acetylation pattern at the *SMN* promoter using chromatin immunoprecipitation with primer-probe sets mapped at ~500 bp intervals along the promoter and first exon. We mapped promoter histone acetylation in mouse neuronal cells, in human fibroblast cells from SMA patients, and in mouse brain, spinal cord, liver and kidney tissues. Although HDAC inhibitors have been previously to increase *SMN* promoter activation, their specific mechanism of action remains poorly understood. We therefore characterized changes in histone acetylation within the SMN promoter following treatment with different HDAC inhibitors.

Next, we characterized the developmental pattern of SMN transcript and protein in mice using tissue lysates from brain, spinal cord, liver and kidney extracted from mice at E15, P1, P7, P15 and adult (3 month) time points. We

then investigated a correlation between the developmental decrease in SMN expression and a change in promoter acetylation.

Materials and Methods:

Cell culture and treatment

NSC-34 cells, a mouse motor neuron-neuroblastoma hybrid cell line, were maintained in Dulbecco's Minimal Essential Medium containing 5% heat-inactivated fetal bovine serum, 1% Penicillin-Streptomycin-Gentamicin and 1% Geneticin (Gibco, Carlsbad, CA). These cells are known to express neuronal properties including generation of action potentials, and acetylcholine synthesis, storage and release (37, 38). The cells were stably transfected with a 3.4 kb fragment of the SMN promoter linked to a β-lactamase reporter gene. Cells were split 1:3 every 2-3 days. We also used a fibroblast line derived from a skin biopsy from a SMA patient with 2 copies of the *SMN2* gene (GM03813, Coriell Cell Repositories, Camden, NJ, USA). Fibroblasts were maintained in Minimal Essential Medium containing 15% fetal bovine serum and 1% Penicillin-Streptomycin-Gentamicin. For experiments, cells were treated with media alone or with media containing valproic acid (VPA, Sigma, St. Louis, MO, USA), valpromide (VPM, Katwijk Chemie BV, The Netherlands), or suberoylanalide hydroxamic acid (SAHA, Calbiochem, San Diego, CA, USA) at the appropriate concentration.

Mouse tissue

C57/Black 6 mice (Charles River Labs, Wilmington, MA) were anesthetized with isoflurane and sacrificed by cervical dislocation (P7, P15, and

adult) or decapitation (E15 and P1). Brain, spinal cord, kidney and liver tissues were dissected from the mice at ages E15, P1, P7, P15 and three-four months, and were flash frozen in liquid nitrogen. Tissue was thawed on ice immediately before use for protein extraction, RNA extraction, or chromatin immunoprecipitation.

Promoter activity

SMN2 promoter activity was measured in transfected NSC-34 cells as a function of *β*-lactamase cleavage of a fluorogenic substrate, CCF-2AM (PanVera, Invitrogen, Carlsbad, CA, USA), as previously described (26). Cells were plated 500,000 per well in a 96-well plate in serum-free media with or without valproic acid or valpromide, and incubated for twenty-four hours. *β*-lactamase activity was assayed according to the manufacturer's protocol. Data is presented as a ratio of emission at 460 nm, representing cleaved substrate, over emission at 530 nm, representing uncleaved substrate.

Protein extraction and Western blotting

Protein was homogenized in 1 ml of lysis buffer (50 mM Tris-HCl, 0.1% Nonidet P-40, 0.5% sodium deoxycholate, 150 mM NaCl, 1 mM EDTA [Sigma]) and kept at 4º C throughout the extraction process. Homogenates were centrifuged at 4000 rpm for 10 minutes to reduce the foam, sonicated at 35% power for 5-10 seconds to lyse the cells, then centrifuged again at 14,000 rpm for 30 minutes to separate the protein fraction. Protein concentration was

determined by the BCA Protein Assay Kit (Pierce, Rockford, IL, USA) according to the manufacturer's instructions. Protein lysates (10 mg) were denatured in sample buffer containing β-mercaptoethanol (Sigma) at 95˚C for five minutes, then run on 12% Tris-Glycine gels with SDS Tris-Glycine running buffer (Invitrogen) for approximately 1.5 hours at 125 V. Protein was transferred to nitrocellulose membranes in transfer buffer (Invitrogen) at 25 V for 2 hours. Nonspecific binding was blocked with 5% (w/v) nonfat dry milk in TTBS. Membranes were probed with mouse monoclonal anti-SMN primary antibody at 1:5000 (Transduction Laboratories, San Diego, CA, USA) then goat anti-mouse-HRP secondary antibody at 1:2000 (Santa Cruz Laboratories, Santa Cruz, CA, USA), and developed with the Western Lightning chemiluminescence system according to the manufacturer's protocol (Perkin-Elmer Life Sciences, Oak Brook, IL, USA). Blots were stripped and re-probed with anti-β actin at 1:2000 (Sigma), then stripped and blotted a third time with anti-α tubulin at 1:4000 (Sigma). Density of bands was determined using NIH Image software.

RNA extraction and quantification

Tissue was homogenized in 1 ml TRIzol/50-100mg tissue (Invitrogen) and spun at 12,000 rpm for 10 minutes to separate the low molecular weight nucleic acid fraction. Cells were washed with PBS and suspended in 1 ml TRIzol. RNA was extracted as previously described (26) using 0.2 ml chloroform/ 1 ml TRIzol. After the addition of TRIzol, the samples were vortexed vigorously then centrifuged at 12,000 g for 10 minutes at 4˚C. The aqueous phase was

transferred to a fresh tube with 0.5 ml isopropyl alcohol/1 ml TRIzol. Samples were centrifuged at 12,000 g for 10 minutes at 4˚C and the pellet washed once with 1 ml of 70% ethanol. Samples were purified with the RNAeasy clean-up kit according to the manufacturer's protocol (Qiagen, Valenica, CA, USA). Total RNA was quantified by absorption at 260 nm, and 50-ng/5 µL was loaded into each 25-µL real time, reverse transcriptase-PCR reaction. The level of SMN RNA was quantified by the $\Delta\Delta C_t$ method using 18S as an endogenous control on the ABI Prism 7900 in 96-well plates (Applied Biosystems, Foster City, CA, USA). *SMN* primers and probes were 5' to 3' as follows: SMN forward: GAATGCCACAACTCCCTTG, SMN probe: FAM-CAGTGGAAAGTTGGTGAC-BHQ, SMN reverse: GCAGCCGTCTTCTGACCAA. Each reaction contained 12.5-µl 2X-reaction buffer, 0.9 µl $MgSO_4$, 1.25 µl of 20X ABI primer-probe mix, 3.1 µl Rox reference dye, 1.75 µl dH_2O, 0.5 µl SS-RT Taq, and 5 µl of sample. Cycling parameters were: 30 minutes at 45 C and five minutes at 95 C, then 50 cycles of 15 seconds at 95 C, 1 minute at 60 C.

Chromatin immunoprecipitation

Chromatin immunoprecipitation (ChIP) was performed on cells and tissue homogenates as previously described (39-41) using 10 ug of antibody to acetylated histone subunit H3 (ARTKQTAR $_{Ac}$KSTGG $_{Ac}$KAPRKQLC) or acetylated histone subunit H4 (AGG $_{Ac}$KGG $_{Ac}$KGMG $_{Ac}$KVGA $_{Ac}$KRHS-C) (Upstate, Lake Placid, NY, USA). In cell experiments, each condition required three 150 mm plates of confluent NSC-34 cells, or twelve 150 mm plates of

fibroblasts. Proteins and DNA in each sample were reversibly cross-linked with 1% formaldehyde (Sigma), 10-mL/150mm plate of cells or 10 µL/mg of tissue, for 10 minutes at 37˚C. Formaldehyde was neutralized by incubation with 1:20 2.5 M glycine at 37˚C for ten minutes (0.5mL/10mL/150mm plate).

Samples were washed three times in 2 ml ice-cold PBS and incubated for 10 minutes on ice in ChIP lysis buffer (1% SDS, 10 mM EDTA, 50 mM Tris-HCl pH 8.1). For *in vitro* experiments, cell plates were taken to a cold room (4 C), where each plate was washed three times in 2 ml ice-cold PBS. Two milliliters of ChIP lysis buffer was then added to each plate and the cells were scraped off the plate into the buffer. The cells, now suspended in buffer, were transferred to three 1.5 ml eppendorf tubes for sonication, 500 µl per tube. DNA was sheared by sonication (8 x 15 sec.) yielding 0.5-1 kb fragments of DNA. Sonication efficiency was evaluated in each experiment by running the sonicated chromatin on a 1% agarose gel. The concentration of each sample was determined by uncrosslinking 5 µl of sample for one hour at 65˚C in uncrosslinking solution (190 µl lysis buffer containing 40 mM NaCl + 5 µl proteinase K = 5 µl sample), then reading the optical density at 260 nm. Samples were diluted a minimum of 1:10 in ChIP dilution buffer (0.01% SDS, 1.1% Triton X-100, 1.2 mM EDTA, 16.7 mM NaCl) to the same final concentration. Chromatin was pre-cleared with 100 µl of salmon sperm agarose A beads per 6 ml chromatin for one hour at 4˚C. After centrifuging at 800 rpm for one minute and removing the chromatin to a fresh tube, 50 µL of chromatin was removed to use as an input control and stored at -80˚C. For each immunoprecipitation, 1.9 ml of chromatin was incubated

overnight at 4˚C with the antibody of choice, or with no antibody (cells) or nonspecific IgG (tissue) as a control. Chromatin and antibody were then incubated with 60 µL of salmon sperm agarose A beads for 1 hour and spun down at 800 rpm for 1 minute. Each sample was washed for 5 minutes each in low salt (0.1% SDS, 1% Triton X-100, 2mM EDTA, 20 mM Tris-HCl pH 8.1, 150 mM NaCl), high salt (0.1% SDS, 1% Triton X-100, 2 mM EDTA, 20 mM Tris-HCl pH 8.1, 500 mM NaCl), lithium chloride (0.25 M LiCl, 1% Nonidet P-40, 1% deoxycholate, 1 mM EDTA, 10 mM Tris-HCl pH 8.1) and 2 x TE (10 mM Tris-HCl, 1 mM EDTA pH 8.0) buffers with 1 min x 800 rpm centrifugation to remove each wash. Chromatin was eluted using 1% SDS in water (250 µl 1% SDS x 15 minutes at room temperature on rotation). The beads were centrifuged down (1000 rpm x 1 minute), and the elute was removed to a fresh tube with 1 ml insulin needles in order to remove all the elute without disturbing the pellet of beads. Elution was repeated in 250 µl 1.5% SDS, and the elute was again removed with 1 ml insulin needles and combined with the 1% SDS elute. Input samples were thawed and brought to equal volume with 225 µl each of 1% and 1.5% SDS solution. Samples and inputs were uncrosslinked in uncrosslinking solution (20 µl Tris-HCl pH 6.5, 20 µl 5 M NaCl, 10 µl 0.5M EDTA, 5 µl proteinase K) at 65˚ C overnight. DNA was extracted with an equal volume (500 µl) of phenol: chloroform: isoamyl alcohol, 1:1:50, in a gel phase-lock tube (Brinkmann Instruments, Eppendorf, Germany) and separated at 14,000 rpm x 15 minutes at room temperature. The organic layer was transferred to two fresh tubes, 250 µL each, with 3 volumes (750 µL) of 100% ice-cold ethanol. After centrifuging at

14,000 rpm for 30 minutes, pellets were washed once in 150 µL of 70% ethanol, air-dried for one hour, and resuspended in PCR-grade ddH_2O.

Real time PCR with a standard curve was used to quantitate relative amounts of DNA. A standard curve for the human gene was generated from the plasmid containing the human *SMN2* promoter used to transfect the NSC-34 cells (Vertex Pharmaceuticals, Cambridge, MA, USA). Mouse experiments used a standard curve generated from dilutions of whole mouse genomic DNA (Santa Cruz Biotechnology). Two separate sets of primers and standards were designed for analysis of the human and mouse promoters (Figure 1). Primers and probes were designed to amplify six regions of the human *SMN2* promoter, labeled here as HuSP1 (for human *SMN* promoter), HuSP2, HuSP3, and HuSP4 (Biosource, Camarillo, CA, USA) or six regions of the mouse *SMN2* promoter and exon 1, labeled here as MSP0 (for mouse *Smn* promoter), MSP1, MSP2, MSP3, MSP4 and MSP5 (see Table 1). Primers for the mouse beta-globin major gene were 5' to 3' as follows: forward: AGGTGAGGTAGGATCAGTTGCTPCR, probe: ACTATGTCAGAAGCAAATGT, reverse: GTGCACCATGATGTCTGTTTCTG. PCR reactions contained an Invitrogen master mix (2.5 µL 10X platinum buffer, 1.75 µL 50 mM $MgCl_2$, 0.5 µL 10mM dNTP, 1.25 µL of 20X ABI primer-probe mix, 3 µL Rox, 0.125 µL platinum Taq, 11.825 µL dH_2O and 5 µL sample), or an ABI master mix (12.5 µL 2X Universal Master Mix, 1.25 µL of 20X ABI primer-probe mix, 6.25 µL dH_2O). PCR cycling conditions were: 5 minutes ramping at 95 C, then 40 cycles of 15 seconds at 95

C, 1 minute at 60 C. After subtracting the baseline no antibody control, values are expressed as a ratio over the input for each experimental condition.

Results

The SMN gene has a characteristic pattern of histone acetylation

The chromatin immunoprecipitation assay, known as ChIP, is able to measure protein interactions with specific regions of DNA in the native chromatin environment. We used ChIP coupled with real time-PCR to measure the level of acetylated H3 and H4 histones associated with the *SMN* promoter and gene.

We first examined the histone acetylation pattern of the mouse *Smn* gene in NSC-34 cells, a cell line derived from mouse motor neurons crossed with neuroblastoma cells (Figure 2). This line was chosen for its motor neuron characteristics, including the ability to generate action potentials, and to synthesize, store and release acetylcholine (37, 38). For comparison of acetylation levels, we used the transcription site region of the mouse β-globin gene. Histone acetylation is well described at this locus as being relatively hypoacetylated in tissues where the gene is silent, and hyperacetylated in erythroid precursor cells, where the gene is expressed at high levels (42). We found that the regions surrounding the *Smn* transcriptional initiation site, designated MSP3 and MSP4 in the mouse genome, were associated with the highest levels of acetylated H3 and H4 histones, in comparison to the regions ~1.3-3.5 kb upstream, and ~1kb downstream. The hypoacetylated regions of the *Smn* promoter had comparable levels of histone acetylation to the β-globin gene, which is transcriptionally silent in this cell type. We next examined the transgenic human *SMN2* promoter and gene, stably transfected randomly into the genome

of the NSC-34 cell line, and found the same pattern of increased acetylation in the region of the transcription site, designated HuSP3 and HuSP4, and less acetylation in regions further upstream.

In order to examine the human *SMN* gene in its native chromatin environment, we performed ChIP experiments on fibroblast cell lines derived from skin biopsies of spinal muscular atrophy patients. In particular, we used the 3813 line from a patient with type I SMA, known to have 2 copies of *SMN2* and deletions in the region of exons 7 and 8 in both copies of *SMN1*. A similar pattern was seen at the *SMN* promoter in the fibroblasts, as was observed in the transgenic *SMN2* in the NSC-34 cells. H3 and H4 acetylation were increased at HuSP3 and HuSP4 compared to the rest of the *SMN* promoter sequence and to the *β-globin* gene transcription locus. Similar preliminary results were obtained from fibroblast cell lines 9677 and 2906, derived from patients with SMA type I and II, no *SMN1*, and with two and four copies of *SMN2*, respectively (data not shown).

Histone deacetylase inhibitors activate the SMN promoter

Histone deacetylase (HDAC) inhibitors have been previously shown to activate the *SMN2* promoter *in vitro* (26, 29), and have been used in limited clinical trials as a therapy for spinal muscular atrophy (21). However, these agents change the expression of ~2% of genes, and it is unknown whether they are acting directly at the *SMN* promoter site. We therefore investigated changes

in H3 and H4 histone acetylation within the *SMN* promoter region following HDAC inhibitor treatment in NSC-34 and 3813 fibroblast cell lines.

We first confirmed *SMN2* promoter activation by treating NSC-34 cells with various drugs for 24 hours and measuring promoter activity (Figure 3). The vector stably transfected into the NSC-34 cells contains the 3.4kb putative *SMN* promoter coupled to a β-lactamase gene, such that promoter activation can be measured as a function of cleavage of a fluorogenic substrate by β-lactamase. We found that valproic acid (VPA) increased promoter activation in a dose-dependent manner, with a maximum effect of 1.8-fold increased activation over untreated cells observed at 2.5 mM VPA, as previously described (26, 29). Valpromide (VPM), a structural analog of valproic acid lacking HDAC inhibitory activity did not increase *SMN* promoter activation. Suberoyl anilide hydroxamic acid (SAHA) also increased *SMN2* promoter activity in a dose-dependent manner by a maximum 2-fold at a concentration of 1 μM. Similar results have been shown for other HDAC inhibitors (26). Valproic acid has also been shown to increase SMN RNA and SMN protein in SMA patient fibroblast cell lines (26).

In order to test whether activation of the *SMN2* promoter by HDAC inhibitors is correlated with a change in histone acetylation, we treated NSC-34 cells for 24 hours with 0, 0.5 or 1.0 μM SAHA, then used ChIP coupled with real time PCR to measure H3 and H4 histone acetylation (Figure 4). We found that SAHA increased histone acetylation specifically within the upstream regions hypoacetylated at baseline (HuSP1, HuSP2), but not in the downstream regions hyperacetylated at baseline (HuSP3, HuSP4) (Figure 7). A maximum 2.3 fold

increase in H3 histone acetylation over mock treated cells was observed at the HuSP1 site after treatment with 0.5 μM SAHA, with no increase observed at HuSP4. A maximum 3.3 fold increase in H4 histone acetylation over mock treated cells was observed at the HuSP1 site with 1.0 μM SAHA treatment. An apparent 1.4 fold increase in H4 histone acetylation was observed at HuSP4 at this same concentration. We also treated 3813 fibroblasts with the HDAC inhibitor valproic acid for four hours (based on earlier time trial experiments). Although these data are not conclusive, we observe a maximum 4.4 fold increase in H3 acetylation at HuSP2 with 5 mM VPA treatment, and a maximum 4.5 fold increase in H4 acetylation at HuSP1 with 5 mM VPA treatment.

Smn *gene expression is developmentally down-regulated*

Previous investigators have described a decrease in SMN protein levels with development (18, 43-45), although this effect has never been well-characterized at the mRNA level. Using samples of brain, spinal cord, kidney and liver tissue, we measured Smn protein and RNA from three animals at each time point: E15, P1, P7, P15, and adult (three-four months).

For use in Western blots, protein isolates were quantified in triplicate in two separate assays, and band densities were compared to both α-tubulin and β-actin (Figure 5A,B). Neither actin nor tubulin was expressed consistently across tissue types, with actin significantly less expressed in embryonic liver. In our assay, we observed a 50-85% decrease in Smn protein in every tissue type between embryonic and adult time periods, consistent with previous descriptions

of Smn in development. Interestingly, embryonic liver reliably showed a second, smaller Smn protein species not seen in other tissues and not previously reported in human fetal liver (8). This species was present with different Smn antibodies, and was not present as non-specific staining (data not shown).

In order to better quantify the change in *Smn* expression during development in different tissues, and to investigate whether this change was due to transcriptional or post-translational mechanisms, we measured Smn RNA by reverse transcriptase real time PCR (Figure 5C). Transcript levels were analyzed by the $\Delta\Delta C_t$ method using two different endogenous controls, 18S and β-2-microglobulin, for comparison. Overall, a ~40-60% decrease in Smn RNA was observed in every tissue between E15 and adult ages when compared to 18S RNA (presented here), and an ~85-95% decrease was observed when compared to β-2-microglobulin. Because 18S was found to increase slightly with development, the effect shown in the graph is slightly less than the true change measured by Smn alone. β-2-microglobulin, by contrast, increased slightly with development, overestimating the change in Smn transcript (data not shown). In liver, the level of Smn RNA was 30-35% of the other tissues at each time point, consistent with the lower levels of Smn protein seen in the Western blots.

Interestingly, all three spinal cord samples were significantly lower than the other two tissues at the P1 time point. Although there was more variation between individual animals at the adult time point, our data suggest that in the neural tissues (spinal cord and brain) there is a small increase in Smn expression

after the nadir observed at P15, a change that is not present in the non-neural tissues (liver and kidney).

Histone acetylation of the SMN *promoter during development*

In order to investigate whether histone acetylation plays a role in regulating *SMN*/*Smn* expression *in vivo*, we looked for a change in histone acetylation associated with the developmental down-regulation of the *Smn* gene. We again used chromatin immunoprecipitation coupled to real time PCR to examine histone H3 and H4 acetylation at six points along the mouse *Smn* promoter and intron 1 in neural (brain) and non-neural (liver) tissue from E15 and adult mice (Figure 6). Spinal cord could not be used because the quantity of tissue obtained from the embryonic mice was insufficient. For each chromatin preparation, roughly 0.2 mg of tissue was used, requiring up to 6-8 individuals in the case of embryonic brain to reach sufficient quantity of material for the assay. Each point is the average of at least three chromatin preparations from different animals, run in triplicate on each of three 384-well PCR plates.

Similar to the pattern of histone acetylation observed in NSC-34 and fibroblast cell lines, we found that in both liver and brain, the regions immediately upstream of the transcription initiation site, MSP3 and MSP4, were relatively hyperacetylated compared to regions further upstream in the promoter (MSP0-2), and further downstream within the transcribed region (MSP5). This pattern was conserved between brain and liver, and between developmental time points. In both tissues, we found that H3 and H4 histone acetylation were approximately

ten times greater in the most acetylated region, MSP4, than in the least acetylated regions of MSP0, 1, and 2.

When comparing embryonic to adult liver tissue, acetylation of histones H3 and H4 decreased at the MSP4 site by 34% and 38% respectively, corresponding to a 66% decrease in Smn transcript. In brain, H3 and H4 acetylation decreased by 21% and 7% respectively, corresponding to a 40% decrease in SMN transcript. Generally, little or no change was observed at other sites, except MSP3 and MSP5 where an increase in acetylation was observed, primarily limited to H4 in liver. For comparison, we also measured histone acetylation at the transcription initiation site of the mouse *β-globin* gene. We found that in embryonic liver, a major site of hematopoesis, acetylation of the *β-globin* gene is comparable to hyperacetylated regions of the *Smn* promoter. Between E15 and adult samples, acetylation of H3 and H4 histones at the *β-globin* gene decreased by 88% and 76%, respectively, corresponding to a >99% decrease in transcript levels. In brain, where the *β-globin* gene is not expressed at any point in development, acetylation of the *β-globin* gene is equivalent to adult liver and to upstream hypoacetylated regions of the *Smn* promoter.

Discussion

Spinal muscular atrophy is an inherited motor neuron disease for which there is currently no treatment. It is caused by mutation or deletion of *SMN1*, leading to insufficient quantities of full length SMN protein. One promising therapeutic strategy has been increasing expression of the *SMN2* gene using histone deacetylase (HDAC) inhibitors. HDAC inhibitors have previously been shown to activate the *SMN2* promoter, and to increase SMN mRNA and protein levels (26, 29). However, the mechanism of action for the effects observed with HDAC inhibitors is not understood, and the role of histone acetylation in directly regulating *SMN* expression has never been explored. Here, we use chromatin immunoprecipitation to look at baseline histone acetylation within the *SMN/Smn* promoter, and then investigate changes in that baseline associated with gene expression changes. We show for the first time that histone acetylation within the *SMN/Smn* promoter changes in a site-specific manner following HDAC inhibitor treatment *in vitro*, and in association with developmental down-regulation of the gene *in vivo*.

First, a characteristic pattern of histone acetylation is established which is conserved across cell lines, species, and tissue types. Histones associated with the translational initiation site are hyperacetylated at both H3 and H4 histone tails, compared to regions >1 kb upstream, or downstream within exon 1. This pattern is consistently observed in mouse motor neuron cells, both in the mouse endogenous gene and the human transgene, in human fibroblasts derived from

SMA patients, and in mouse tissue from brain, spinal cord, liver, and kidney in both embryonic and adult mice. This pattern of greater histone acetylation surrounding the initiation site is consistent with other active genes studied, for example, in the active human *interferon-β* (35) and mouse *β-globin* genes (46). In genome wide studies of yeast and Drosophila, histones in the 5' transcribed region of active genes are generally hyperacetylated compared to histones within the gene or in more distant regulatory sequences (36, 47).

Interestingly, this region immediately surrounding the translation initiation site, is the region previously identified as the minimal functional promoter region (19). More recently, Rouget *et al.* refined the minimal functional promoter sequence to 15 bp upstream and 117 bp downstream of the transcriptional start site for the human *SMN* gene, and 46 bp upstream and 125 bp downstream of the transcriptional start site for the mouse *Smn* gene. In their work, inclusion of upstream sequence in promoter constructs reduces promoter activity, suggesting that upstream regions may be involved in repressor activity (32). This is supported by Boda *et al.* who found regions with repressor activity as far as 4.6kb upstream (33).

The sequence of the core promoter region is conserved between the mouse and the human genomes, and contains binding sites for numerous transcription factors, including cAMP-response element binding protein (CREB) and Sp (32, 48). The CREB family of transcription factors, in particular, is known to recruit the highly potent histone acetyltransferase, p300/CREB binding protein

(CBP) (49), suggesting that recruitment of p300/CBP to the *SMN* promoter could be responsible for the high acetylation levels observed in this region.

Next, the 1.7 to1.9- fold increase in *SMN/Smn* promoter activity previously observed with HDAC inhibitor treatment (valproic acid and SAHA), is found to correspond with an increase in H3 and H4 histone acetylation within the *SMN/Smn* promoter region. According to our data, histone deacetylase inhibitors have a specific effect on the acetylation of H3 and H4 histones located further upstream at sites hypoacetylated at baseline, and no measurable effect on histones associated with the translational initiation site. These data suggest that HDAC inhibitors do have an effect within the region of the *SMN* promoter, but not at the transcription site, raising the question of whether the HDAC-induced *SMN* promoter activation is a direct effect, or secondary to upregulation of some other molecule, such as a transcription factor. Alternatively, it is known that HDACs not only deacetylate histones but also non-histone proteins that are transcriptional regulators (30). Thus, HDAC inhibitor treatment could result in acetylation and activation of a DNA binding factor that recruits HATs and leads to acetylation of the *SMN2* gene in upstream regions.

In order to examine the biological significance of histone acetylation in regulation of *SMN/Smn* expression, experiments were shifted to an *in vivo* system, mouse tissue from different developmental time points. Although SMN protein has long been known to be developmentally down-regulated (18), we present the first rigorous quantitation of this effect at the mRNA level. A 40-60% decrease in SMN RNA is seen in all tissues between E15 and adult (three

month) mice. Interestingly, both the SMN protein and RNA are lower in liver tissue, 30-35% of other tissues, at every developmental time point. The significance of this finding is not known. One limitation of our study is the use of whole tissue lysates. It has been show by *in situ* hybridization that the distribution of SMN in the spinal cord changes with development from being more diffuse to being specifically concentrated in motor neurons (50), an effect which is not appreciated in our method. Of note, we found that SMN levels in the spinal cord dropped significantly more than other tissues at the P1 time point (~20%), suggesting that down-regulation of SMN may take place earlier in spinal cord than in other tissues, and may therefore be subject to different regulatory mechanisms. Recently, this finding was corroborated in experiments using sucrose centrifugation followed by western blot, in which the authors show that the decrease in SMN RNA corresponds to the process of myelination in the spinal cord, which occurs earlier than in the brain (51).

Finally, we correlated this developmental change in expression with a change in histone acetylation within the *Smn* promoter. At the MSP4 site, the region closest to the transcriptional and translational initiation sites, we observed a decrease in acetylated H3 and H4 levels in liver tissue, and a decrease in H3 acetylation in brain tissue. This was associated with a 40-60% decrease in *Smn* mRNA, as measured by real time RT-PCR. Although the observed decrease in acetylation is modest, studies in other genes have noted similarly small changes in acetylation associated with large changes in gene expression. The mouse β-globin gene is perhaps the best studied, in which gene induction produced only a

two-fold increase in H3 acetylation in association with a 150-fold increase in expression. Within neighboring regions in the *Smn* promoter and gene, MSP5 and MSP3, small increases in H3 and H4 acetylation were observed. However, we believe the decrease at MSP4 is the most relevant as this is the most transcriptionally active region of the gene. Furthermore, in more recent experiments, this developmental, regionally specific decrease in acetylation has been associated with a large increase in HDAC2 and a smaller increase in HDAC1 within the same region (52).

Although chromatin immunoprecipitation is a powerful technique, its limit of detection does not extend below 500 bp. Thus the alternate transcription recently described by Rouget *et al.* as a site used preferentially during development could not be distinguished in our work, as it is only 79 bp away from the adult transcription initiation site (32). It may be that histone acetylation changes locally within regions smaller than our 500 bp limit of detection.

There has been some controversy in the literature about the use of HDAC inhibitors as a treatment for spinal muscular atrophy, in particular because of their lack of specificity, requirements for high doses, and as yet poorly understood site of action. As mentioned previously, HDAC inhibitors affect the expression of approximately 2% genes. They also seem to act on most of the known class I and II HDACs, including those HDACs that act on non-histone proteins and are located predominantly outside the nucleus (30). HDAC inhibitors have also been explored for their ability to change the expression of numerous other genes, including tumor suppressor and oncogenes (reviewed in

(53), so there is a theoretical risk of activating repressed oncogenes and increasing the incidence of cancer. Valproic acid is used as an anti-epileptic medication because of its effect on sodium channels, at a maximum dose of 60 mg/kg/day resulting in serum levels of 50 -100 μg/ml. Even at this dose, which is lower than the dose required for HDAC inhibition, valproic acid is a known teratogen and can cause numerous side effects, including mental status changes. It has been postulated that HDAC inhibition increases *SMN* expression by increasing histone acetylation at the SMN promoter, and although the data presented here support this idea, this has not been proven. Given the need for high doses, and the poorly understood, nonspecific nature of our current arsenal of HDAC inhibitors, long-term treatment with high doses of these drugs is likely to cause significant immediate and long term side effects, and we cannot predict what these will be.

To address some of these questions, experiments are underway to test the safety and feasibility of HDAC inhibitor treatment in a mouse model of spinal muscular atrophy. Further ChIP experiments are also underway using antibodies against individual HDACs, particularly those in class I, which are concentrated in the nucleus, in order to determine which particular HDACs may be acting at the *SMN* promoter locus. ChIP can also be used to determine other proteins present at the *SMN* promoter, for example bound transcription factors or histone acetyltransferases (HATs). Also important will be to determine the relative activity of particular inhibitors against individual HDACs, and whether more specific inhibitors can be developed to target the HDACs active in controlling

SMN. Together these experiments may allow more specific targeting of the histone acetylation machinery at the *SMN* gene locus.

The histone acetylation system described here is only one of the many epigenetic determinants that may be relevant to the expression of *SMN*. Methylation, phosphorylation and sumoylation are well-described histone modifications known to affect gene expression individually, and to interact with histone acetylation in controlling gene expression (24, 54). In addition to affecting immediate transcription factor binding and chromatin accessibility, histone acetylation is also known to influence long term expression controls such as DNA methylation. Methylated DNA and the methylation-specific transcription repressor, MeCP2 have been shown to recruit histone deacetylases (55). Conversely, treatment with the HDAC inhibitor Trichostatin A, has been reported to induce loss of methylation at specific genes (56). Further, a number of heavily methylated genes studied *in vitro* have been reported to be unresponsive to the HDAC inhibitor Trichostatin A without pretreatment with a demethylating agent (reviewed in (57). These data suggest that treatment with a demethylating agent plus an HDAC inhibitor may increase the expression of *SMN* beyond what each agent can do individually. The effect may even be synergistic, and could allow the use of lower doses of HDAC inhibitors in the treatment of spinal muscular atrophy. Further experiments investigating the contributions of other epigenetic determinants, particularly DNA methylation, may therefore be warranted.

In conclusion, we have shown that *SMN* has a reproducible pattern of histone acetylation that is modified by HDAC inhibitor treatment and during the course of development. Together, these data strongly suggest that histone acetylation plays an important role in *SMN*/*Smn* regulation and that this epigenetic determinant can be manipulated pharmacologically. However, this work represents a proof of concept, and significant work will be required before we can hope to exploit this knowledge to have an impact on the course of the disease. In particular, future experiments should concentrate on investigating how to more specifically target the histone acetylation machinery at the *SMN* locus, and how other epigenetic systems might be exploited to further increase *SMN* expression.

References

1. Crawford TO, Pardo CA. The neurobiology of childhood spinal muscular atrophy. Neurobiol Dis 1996;3(2):97-110.

2. Ogino S, Wilson RB. Spinal muscular atrophy: molecular genetics and diagnostics. Expert Rev Mol Diagn 2004;4(1):15-29.

3. Jablonka S, Sendtner M. Molecular and cellular basis of spinal muscular atrophy. Amyotroph Lateral Scler Other Motor Neuron Disord 2003;4(3):144-9.

4. Swoboda KJ, Prior TW, Scott CB, et al. Natural history of denervation in SMA: relation to age, SMN2 copy number, and function. Ann Neurol 2005;57(5):704-12.

5. Briese M, Esmaeili B, Sattelle DB. Is spinal muscular atrophy the result of defects in motor neuron processes? Bioessays 2005;27(9):946-57.

6. Schmalbruch H, Haase G. Spinal muscular atrophy: present state. Brain Pathol 2001;11(2):231-47.

7. Iannaccone ST, Smith SA, Simard LR. Spinal muscular atrophy. Curr Neurol Neurosci Rep 2004;4(1):74-80.

8. Lefebvre S, Burglen L, Reboullet S, et al. Identification and characterization of a spinal muscular atrophy-determining gene. Cell 1995;80(1):155-65.

9. Monani UR, McPherson JD, Burghes AH. Promoter analysis of the human centromeric and telomeric survival motor neuron genes (SMNC and SMNT). Biochim Biophys Acta 1999;1445(3):330-6.

10. Lorson CL, Androphy EJ. An exonic enhancer is required for inclusion of an essential exon in the SMA-determining gene SMN. Hum Mol Genet 2000;9(2):259-65.

11. Lorson CL, Hahnen E, Androphy EJ, Wirth B. A single nucleotide in the SMN gene regulates splicing and is responsible for spinal muscular atrophy. Proc Natl Acad Sci U S A 1999;96(11):6307-11.

12. Gubitz AK, Feng W, Dreyfuss G. The SMN complex. Exp Cell Res 2004;296(1):51-6.

13. Paushkin S, Gubitz AK, Massenet S, Dreyfuss G. The SMN complex, an assemblyosome of ribonucleoproteins. Curr Opin Cell Biol 2002;14(3):305-12.

14. Rossoll W, Kroning AK, Ohndorf UM, Steegborn C, Jablonka S, Sendtner M. Specific interaction of Smn, the spinal muscular atrophy determining gene product, with hnRNP-R and gry-rbp/hnRNP-Q: a role for Smn in RNA processing in motor axons? Hum Mol Genet 2002;11(1):93-105.

15. Zhang HL, Pan F, Hong D, Shenoy SM, Singer RH, Bassell GJ. Active transport of the survival motor neuron protein and the role of exon-7 in cytoplasmic localization. J Neurosci 2003;23(16):6627-37.

16. Fan L, Simard LR. Survival motor neuron (SMN) protein: role in neurite outgrowth and neuromuscular maturation during neuronal differentiation and development. Hum Mol Genet 2002;11(14):1605-14.

17. Ferri A, Melki J, Kato AC. Progressive and selective degeneration of motoneurons in a mouse model of SMA. Neuroreport 2004;15(2):275-80.

18. La Bella V, Cisterni C, Salaun D, Pettmann B. Survival motor neuron (SMN) protein in rat is expressed as different molecular forms and is developmentally regulated. Eur J Neurosci 1998;10(9):2913-23.

19. Germain-Desprez D, Brun T, Rochette C, Semionov A, Rouget R, Simard LR. The SMN genes are subject to transcriptional regulation during cellular differentiation. Gene 2001;279(2):109-17.

20. McWhorter ML, Monani UR, Burghes AH, Beattie CE. Knockdown of the survival motor neuron (Smn) protein in zebrafish causes defects in motor axon outgrowth and pathfinding. J Cell Biol 2003;162(5):919-31.

21. Mercuri E, Bertini E, Messina S, et al. Pilot trial of phenylbutyrate in spinal muscular atrophy. Neuromuscul Disord 2004;14(2):130-5.

22. Allfrey VG. Structural modifications of histones and their possible role in the regulation of ribonucleic acid synthesis. Proc Can Cancer Conf 1966;6:313-35.

23. Pazin MJ, Kadonaga JT. What's up and down with histone deacetylation and transcription? Cell 1997;89(3):325-8.

24. Jenuwein T, Allis CD. Translating the histone code. Science 2001;293(5532):1074-80.

25. Van Lint C, Emiliani S, Verdin E. The expression of a small fraction of cellular genes is changed in response to histone hyperacetylation. Gene Expr 1996;5(4-5):245-53.

26. Sumner CJ, Huynh TN, Markowitz JA, et al. Valproic acid increases SMN levels in spinal muscular atrophy patient cells. Ann Neurol 2003;54(5):647-54.

27. Andreassi C, Angelozzi C, Tiziano FD, et al. Phenylbutyrate increases SMN expression in vitro: relevance for treatment of spinal muscular atrophy. Eur J Hum Genet 2004;12(1):59-65.

28. Chang JG, Hsieh-Li HM, Jong YJ, Wang NM, Tsai CH, Li H. Treatment of spinal muscular atrophy by sodium butyrate. Proc Natl Acad Sci U S A 2001;98(17):9808-13.

29. Brichta L, Hofmann Y, Hahnen E, et al. Valproic acid increases the SMN2 protein level: a well-known drug as a potential therapy for spinal muscular atrophy. Hum Mol Genet 2003;12(19):2481-9.

30. Thiagalingam S, Cheng KH, Lee HJ, Mineva N, Thiagalingam A, Ponte JF. Histone deacetylases: unique players in shaping the epigenetic histone code. Ann N Y Acad Sci 2003;983:84-100.

31. Echaniz-Laguna A, Miniou P, Bartholdi D, Melki J. The promoters of the survival motor neuron gene (SMN) and its copy (SMNc) share common regulatory elements. Am J Hum Genet 1999;64(5):1365-70.

32. Rouget R, Vigneault F, Codio C, et al. Characterization of the survival motor neuron (SMN) promoter provides evidence for complex combinatorial regulation in undifferentiated and differentiated P19 cells. Biochem J 2005;385(Pt 2):433-43.

33. Boda B, Mas C, Giudicelli C, et al. Survival motor neuron SMN1 and SMN2 gene promoters: identical sequences and differential expression in neurons and non-neuronal cells. Eur J Hum Genet 2004;12(9):729-37.

34. DiDonato CJ, Brun T, Simard LR. Complete nucleotide sequence, genomic organization, and promoter analysis of the murine survival motor neuron gene (Smn). Mamm Genome 1999;10(6):638-41.

35. Forsberg EC, Downs KM, Christensen HM, Im H, Nuzzi PA, Bresnick EH. Developmentally dynamic histone acetylation pattern of a tissue-specific chromatin domain. Proc Natl Acad Sci U S A 2000;97(26):14494-9.

36. Roh TY, Ngau WC, Cui K, Landsman D, Zhao K. High-resolution genome-wide mapping of histone modifications. Nat Biotechnol 2004;22(8):1013-6.

37. Cashman NR, Durham HD, Blusztajn JK, et al. Neuroblastoma x spinal cord (NSC) hybrid cell lines resemble developing motor neurons. Dev Dyn 1992;194(3):209-21.

38. Durham HD, Dahrouge S, Cashman NR. Evaluation of the spinal cord neuron X neuroblastoma hybrid cell line NSC-34 as a model for neurotoxicity testing. Neurotoxicology 1993;14(4):387-95.

39. Chakrabarti SK, Francis J, Ziesmann SM, Garmey JC, Mirmira RG. Covalent histone modifications underlie the developmental regulation of insulin gene transcription in pancreatic beta cells. J Biol Chem 2003;278(26):23617-23.

40. Kuo MH, Allis CD. In vivo cross-linking and immunoprecipitation for studying dynamic Protein:DNA associations in a chromatin environment. Methods 1999;19(3):425-33.

41. Braveman MW, Chen-Plotkin AS, Yohrling GJ, Cha JH. Chromatin immunoprecipitation technique for study of transcriptional dysregulation in intact mouse brain. Methods Mol Biol 2004;277:261-76.

42. Kim A, Dean A. Developmental stage differences in chromatin subdomains of the beta-globin locus. Proc Natl Acad Sci U S A 2004;101(18):7028-33.

43. Burlet P, Huber C, Bertrandy S, et al. The distribution of SMN protein complex in human fetal tissues and its alteration in spinal muscular atrophy. Hum Mol Genet 1998;7(12):1927-33.

44. Battaglia G, Princivalle A, Forti F, Lizier C, Zeviani M. Expression of the SMN gene, the spinal muscular atrophy determining gene, in the mammalian central nervous system. Hum Mol Genet 1997;6(11):1961-71.

45. Jablonka S, Schrank B, Kralewski M, Rossoll W, Sendtner M. Reduced survival motor neuron (Smn) gene dose in mice leads to motor neuron degeneration: an animal model for spinal muscular atrophy type III. Hum Mol Genet 2000;9(3):341-6.

46. Parekh BS, Maniatis T. Virus infection leads to localized hyperacetylation of histones H3 and H4 at the IFN-beta promoter. Mol Cell 1999;3(1):125-9.

47. Schubeler D, MacAlpine DM, Scalzo D, et al. The histone modification pattern of active genes revealed through genome-wide chromatin analysis of a higher eukaryote. Genes Dev 2004;18(11):1263-71.

48. Majumder S, Varadharaj S, Ghoshal K, Monani U, Burghes AH, Jacob ST. Identification of a novel cyclic AMP-response element (CRE-II) and the role of CREB-1 in the cAMP-induced expression of the survival motor neuron (SMN) gene. J Biol Chem 2004;279(15):14803-11.

49. Ogryzko VV, Schiltz RL, Russanova V, Howard BH, Nakatani Y. The transcriptional coactivators p300 and CBP are histone acetyltransferases. Cell 1996;87(5):953-9.

50. Pagliardini S, Giavazzi A, Setola V, et al. Subcellular localization and axonal transport of the survival motor neuron (SMN) protein in the developing rat spinal cord. Hum Mol Genet 2000;9(1):47-56.

51. Gabanella F, Carissimi C, Usiello A, Pellizzoni L. The activity of the spinal muscular atrophy protein is regulated during development and cellular differentiation. Hum Mol Genet 2005;14(23):3629-42.

52. Kernochan LE, Russo ML, Woodling NS, et al. The role of histone acetylation in SMN gene expression. Hum Mol Genet 2005;14(9):1171-82.

53. Miyamoto K, Ushijima T. Diagnostic and therapeutic applications of epigenetics. Jpn J Clin Oncol 2005;35(6):293-301.

54. Fischle W, Wang Y, Allis CD. Binary switches and modification cassettes in histone biology and beyond. Nature 2003;425(6957):475-9.

55. Jones PL, Veenstra GJ, Wade PA, et al. Methylated DNA and MeCP2 recruit histone deacetylase to repress transcription. Nat Genet 1998;19(2):187-91.

56. Selker EU. Trichostatin A causes selective loss of DNA methylation in Neurospora. Proc Natl Acad Sci U S A 1998;95(16):9430-5.

57. Dobosy JR, Selker EU. Emerging connections between DNA methylation and histone acetylation. Cell Mol Life Sci 2001;58(5-6):721-7.

Figure 1: Primer/probe sets for PCR of the *SMN/Smn* promoters and genes.

A.

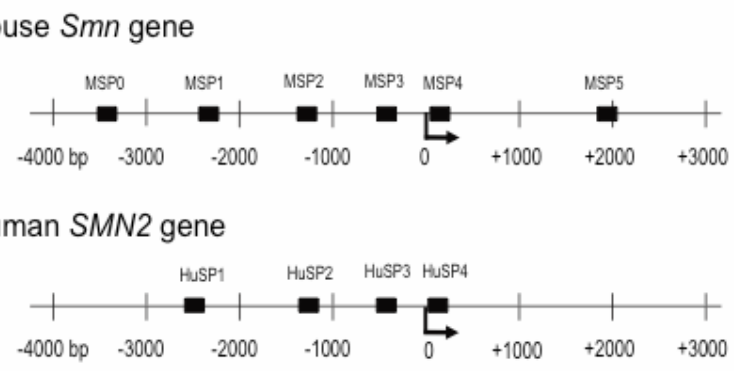

B.

Mouse or Human specific SMN primer/ probe set	Forward primer sequence (5'-3')	Reverse primer sequence (5'-3')	Probe sequence (5'-3')
MSP0	CTTTTAGATGTGTTGTCAAGC TGCTA	ATGAAAGCATTTCTAAGAGGGA AACTCA	CTCTCTCCCGTTTCTTCTTG
MSP1	GGTTCCCGTCCTTGTATTGG TTTT	ACCCATTATCTCTCCACGAATC CA	CCCTTCAAAGGATAATAACA
MSP2	CCTGGCATGGGCGAAGTG	GCGAAAGGTAAACGTAAGAATC CTACTA	ACCATCATCAGAACCC
MSP3	TGGCACATGGGATATCGAAA TTCT	CGACCATTTCCTTCATCTGGC ATAT	TCCTGAGTCTGATTTTCCT
MSP4	AAGCCCCATGACGGAAGTC	CATCGCCATGGCCTGCTA	CCGGCAGCGTCCGTG
MSP5	CCTCAGGTCATACATTTTGTA AAGAAAGAGA	TTTCTAACATAACAGGTCCCAC CAC	CTAAGAAAGCCTCAATGTG
HuSP1	GCAATGCCAAAGGAAACAG	TAATCGTTTTAGAGAGTACAAT TGAATGG	TGGTGGGTGATTAAAATGTTCT GGAGTTTAGATAGTAGTG
HuSP2	TTTTTGTACATTGGCAACATC ATC	CACGAAAGGAACTTTGAGCTC TTC	CATTCTCCCCTTCCTCCACAGA TATTTCTTGT
HuSP3	GGTTTTAAATTCCTAGTAGGA GCTTACATT	GGGTTTCGGCATGTTGCTT	CACACACTGGAGTTCGAGACG AGGCC
HuSP4	CACTCGTAGAAAGCGTGAGA AGTTA	GCTTCTTGGGAGCGGAACAG	AGCGGTCCTCCCGGCCACC

Figure 1: (A) Schematic of the locations of the primer/probe sets, which were spaced at 500-1000 bp intervals. Arrows represent the transcription initiation sites. Translational initiation sites are located at +163 bp for the human gene and at + 160 bp for the mouse gene (16,28). **(B)** Sequences of *SMN/Smn* promoter primer/probe sets (5'-3'). This and subsequent figures are modified from Kernochan *et al.* (52).

Figure 2A: The *SMN/Smn* gene has a characteristic pattern of H3 histone acetylation

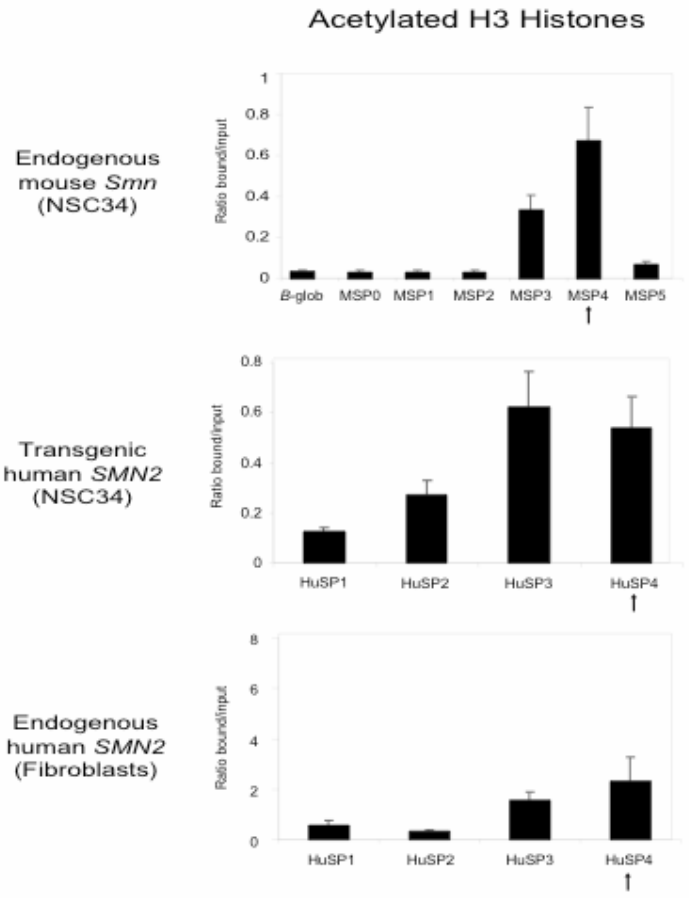

Figure 2: The *SMN/Smn* gene has a characteristic pattern of histone acetylation in which acetylated H3 **(A)** and H4 **(B)** histones are enriched in a restricted region surrounding the transcriptional start site. Using ChIP, the baseline H3 and H4 acetylation patterns were evaluated at the promoters of the endogenous *Smn* gene in NSC-34 cells, the transgenic human *SMN2* gene in NSC-34 cells, and the endogenous human *SMN2* gene in 3813 fibroblasts, isolated from a type I SMA patient. Each value represents the average of three independent chromatin preparations taken from cells harvested on different days (except the HuSP2 site in 3813 fibroblasts, which represents the average of two chromatin preparations). Error bars represent the SEM. The arrow indicates the region closest to the transcription initiation sites of the *SMN/Smn* genes.

Figure 2B: The *SMN/Smn* gene has a characteristic pattern of H4 histone acetylation

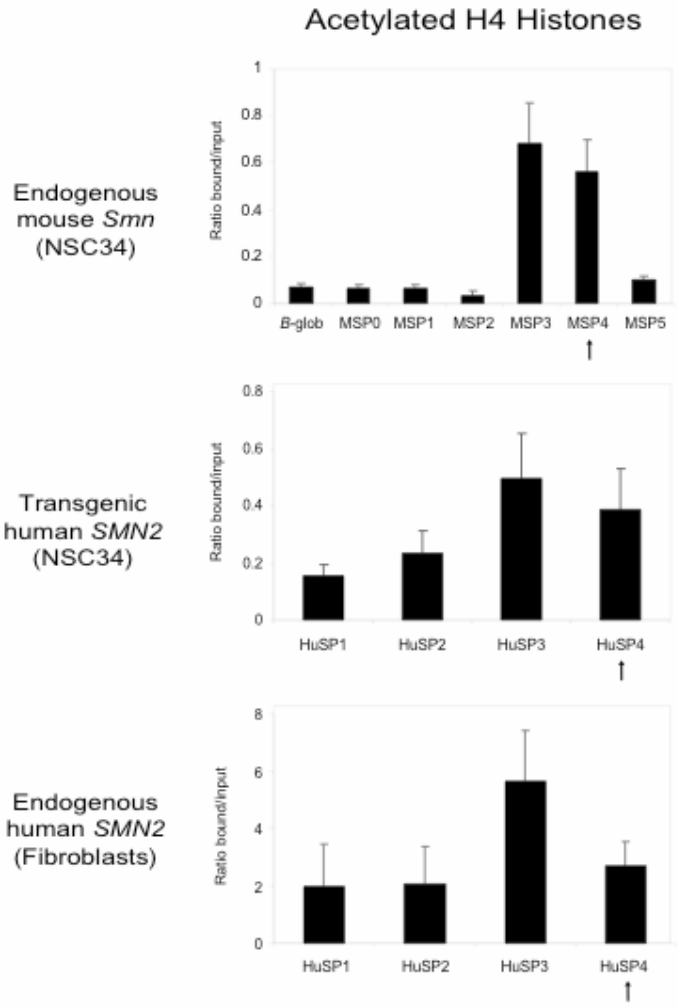

Figure 3: Histone deacetylase inhibitors activate the *SMN2* promoter.

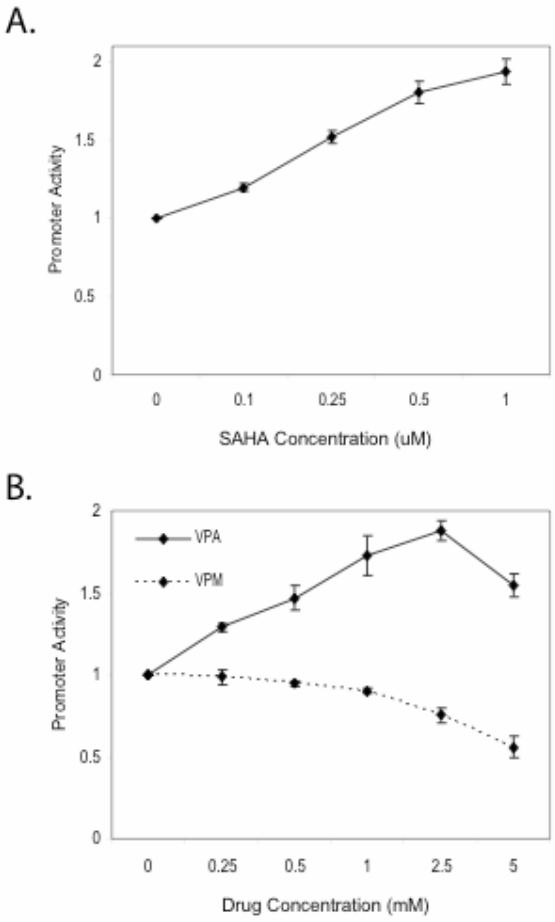

Figure 3: Histone deacetylase inhibitors activate the *SMN2* promoter. *SMN2* promoter activity was measured in NSC-34 cells following 24 hrs. of treatment with **(A)** 0-1 uM suberoylanalide hydroxamic acid (SAHA), or **(B)** 0-5 mM valproic acid (VPA) or valpromide (VPM; a structural analog of VPA lacking HDAC activity). Values are normalized to the untreated sample. Each data point represents the average of three independent experiments. Error bars represent the SEM.

Figure 4A: HDAC inhibitors increase H3 histone acetylation in upstream regions of *SMN2*

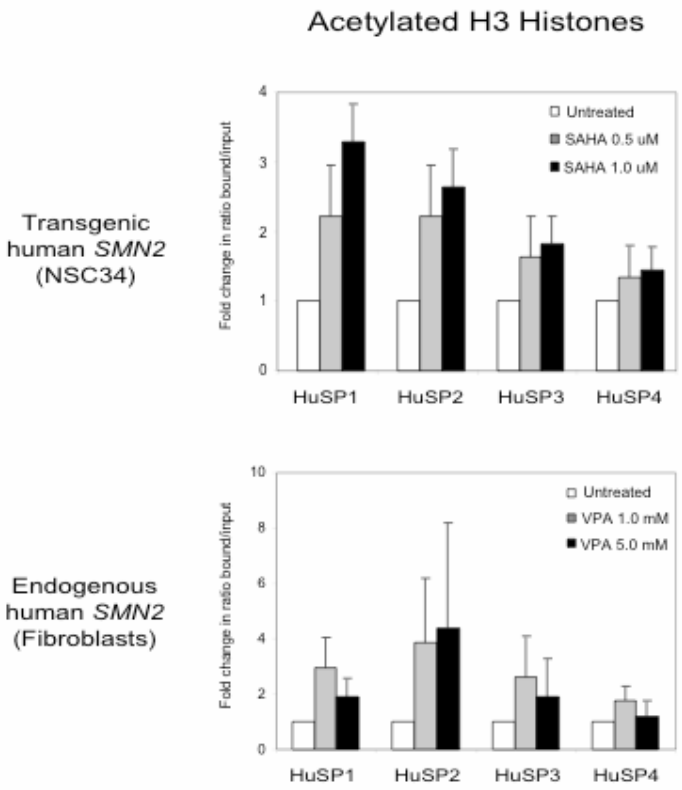

Figure 4: HDAC inhibitors increase H3 **(A)** and **(B)** H4 histone acetylation in upstream regions of *SMN2*. Using ChIP, H3 and H4 histone acetylation levels were measured in NSC-34 cells treated with 0-1.0 uM SAHA for 24 hrs, and 3813 fibroblasts were treated with 0-5 mM VPA for 4 hrs. Each data point represents the average of three independent experiments (except the HuSP2 site in 3813 fibroblasts and the data points for the VPA 1 mM dose, which represent the average of two preparations). Data were normalized to the untreated sample for each gene region. Error bars represent the SEM.

Figure 4B: HDAC inhibitors increase H4 histone acetylation in upstream regions of *SMN2*

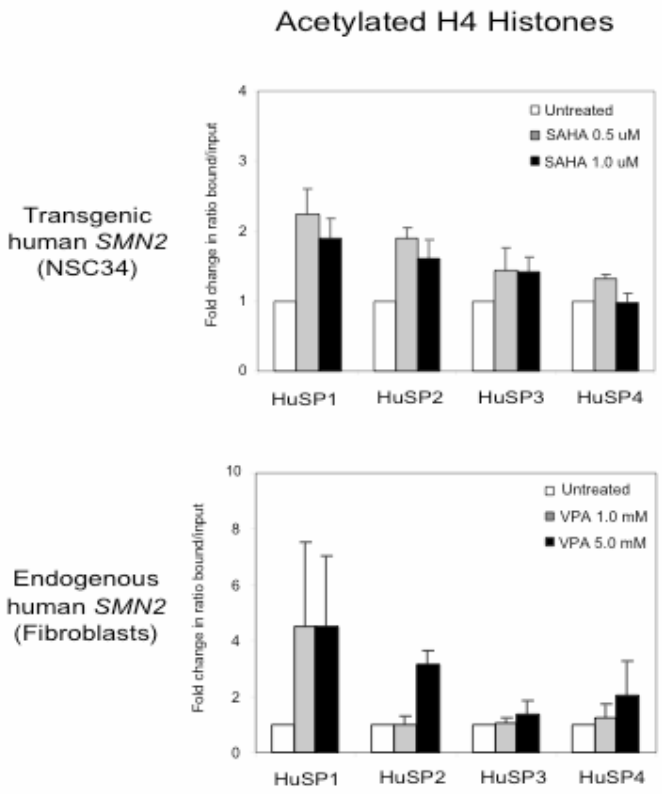

Figure 5A: Smn RNA decreases during development.

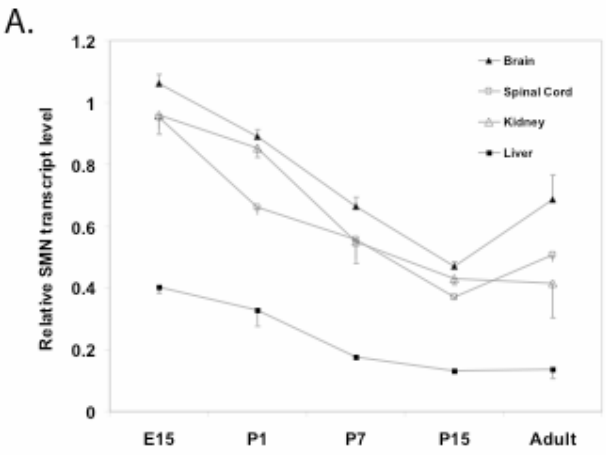

Figure 5: *Smn* gene expression decreases during development. **(A)** Quantitative RT-PCR was used to measure SMN transcript levels in brain, spinal cord, kidney and liver at embryonic day 15, post-natal days 1, 7, and 15, and adult (3 months) time points. Each data point represents the average of 3-4 tissue samples, each from different mice. The data presented used 18S RNA as an endogenous control. All values were normalized to a single E15 brain sample. Error bars represent the SEM. **(B)** A representative western blot showing SMN and actin protein levels in brain, spinal cord (S.C.), kidney, and liver tissues from an E15 mouse, compared to tissues from an adult mouse (3 months). **(C)** Summary of quantification by densitometry of SMN protein levels compared to actin or tubulin loading controls. Each data point represents the average of two sets of protein lysates. Values are normalized to the E15 sample for each set of lysates.

Figure 5B and C: Smn protein decreases during development.

B.

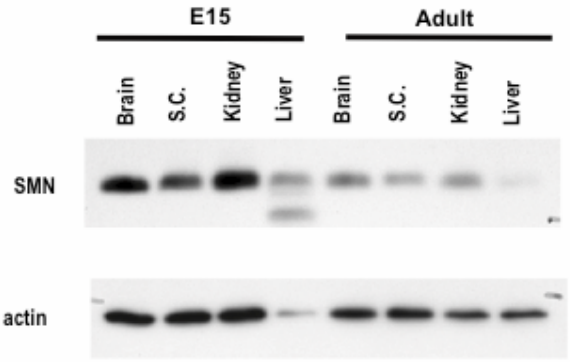

C.

	Brain		Spinal Cord		Kidney		Liver	
	SMN/ actin	SMN/ tubulin	SMN/ actin	SMN/ tubulin	SMN/ actin	SMN/ tubulin	SMN/ actin	SMN/ tubulin
E15	1.0	1.0	1.0	1.0	1.0	1.0	1.0	1.0
P1	1.0	0.6	0.7	0.6	1.0	1.1	0.6	0.2
P7	0.9	0.7	0.7	0.8	0.9	1.1	0.5	0.1
Adult	0.5	0.5	0.3	0.8	0.4	0.5	0.1	0.1

Figure 6A: H3 histone acetylation of the *Smn* promoter decreases during development in the region closest to the transcription initiation site.

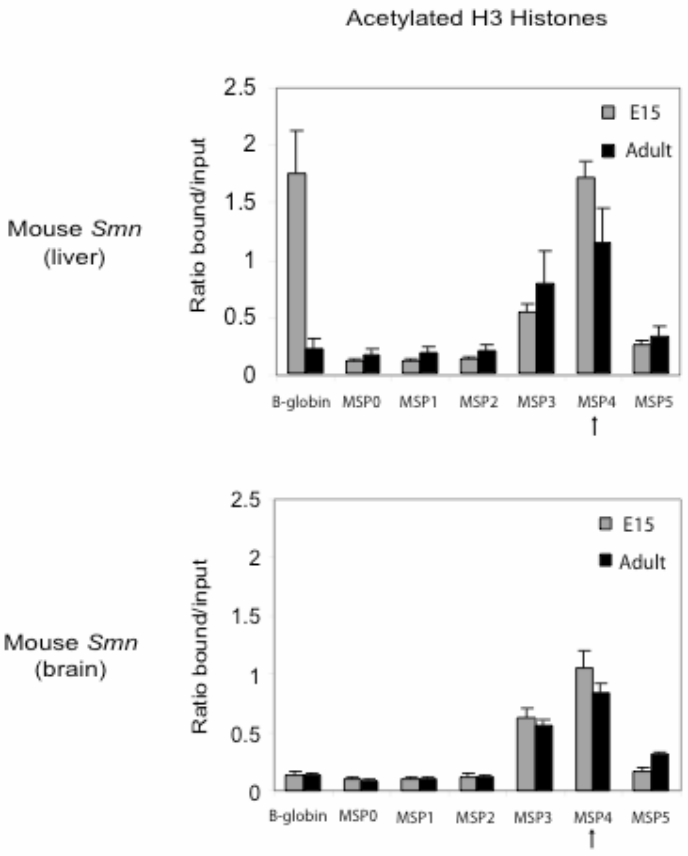

Figure 6: Using ChIP, histone H3 **(A)** and H4 **(B)** acetylation levels were measured at the *Smn* promoter in mouse liver and brain at E15 and adult time points. H3 and H4 acetylation were also measured at the beta-globin gene for comparison. Each value represents the average of three independent chromatin preparations, except embryonic brain, which represents the average of four preparations. Error bars represent the SEM. The arrow indicates the region closest to the transcription initiation site of the *Smn* gene.

Figure 6B: H4 histone acetylation of the *Smn* promoter decreases during development in the region closest to the transcription initiation site.